Available online at www.sciencedirect.com
ScienceDirect
Chemical Physics Letters 435 (2007) 289–294
CHEMICAL PHYSICS LETTERS
www.elsevier.com/locate/cplett

Electron irradiation of crystalline and amorphous D_2O ice

Weijun Zheng [a,b], David Jewitt [a], Ralf I. Kaiser [b,*]

[a] Institute for Astronomy, University of Hawaii at Manoa, Honolulu, HI 96822, United States
[b] Department of Chemistry, University of Hawaii at Manoa, Honolulu, HI 96822, United States

Received 13 October 2006; in final form 4 January 2007
Available online 10 January 2007

Abstract

We studied the electron irradiation of crystalline and amorphous deuterated water ices at 12 K. The experiments show that molecular deuterium (D_2), molecular oxygen (O_2), and Hydrogen peroxide (D_2O_2) were produced inside the irradiated ice samples. A quantitative comparison of crystalline and amorphous ice samples showed that the production rates of D_2, O_2 and D_2O_2 in amorphous ices are systematically higher than those in crystalline samples. Reaction mechanisms and astrophysical implications are discussed.
Published by Elsevier B.V.

1. Introduction

During the last decade, sputtering and irradiation experiments of low temperature water ices have received particular attention [1–6]. These experiments are aimed to understand the interaction of cosmic ray and solar wind particles as well as of ultra violet (UV) photons with ices present in cold molecular clouds, Oort cloud objects, Kuiper Belt Objects, comets, as well as planets and their satellites. One of the prime interests of these studies is to extract formation pathways on how new molecules are formed during the photolysis/irradiation of water ices both qualitatively and quantitatively. Watanabe et al. [7] measured the yield of molecular deuterium (D_2) via ultraviolet irradiation of amorphous water ice (D_2O) at 12 K. Sieger et al. as well as Orlando and Sieger [8,9] unraveled the production of molecular oxygen (O_2) in water ices via electron irradiation exposure. Grieves and Orlando [10] investigated the electron stimulated formation and trapping of D_2 and O_2 in amorphous and crystalline D_2O ices. The generation of hydrogen peroxide inside water ice has been studied recently by various research groups [11–14]. Previous work in our lab suggested that molecular hydrogen, molecular oxygen, and hydrogen peroxide were produced in crystalline water ice via electron irradiation at 12 K [15]. These products were trapped inside the ices until the samples were warmed up. The temperature-dependent studies showed that the production rates of all species decreased as the temperature of the samples is raised [16]. The major component of the icy mantles on the surface of the dust grains in cold molecular clouds and on the surfaces of objects in the Oort cloud is amorphous water ice [17]. Amorphous water ice also exists in comets [18,19]. Therefore, it is necessary to investigate the effects of the porosity and morphology of the ice on the chemical formation routes and on the production rates quantitatively. In this paper, we compare detailed, quantitative studies of the formation of molecular hydrogen, molecular oxygen, and hydrogen peroxide in crystalline and amorphous water ice by energetic electrons.

2. Experimental

In order to eliminate even trace amounts of contamination from water and molecular hydrogen, we conducted our experiments with deuterated water (D_2O, Alfa Aesar, 99.995%). The experiments were carried out in an ultrahigh vacuum chamber (5×10^{-11} Torr) which has been introduced elsewhere [20]. Briefly, a two-stage closed-cycle helium refrigerator coupled with a rotary platform is attached to the main chamber and holds a polished

* Corresponding author.
E-mail address: kaiser@gold.chem.hawaii.edu (R.I. Kaiser).

0009-2614/$ - see front matter Published by Elsevier B.V.
doi:10.1016/j.cplett.2007.01.013

polycrystalline silver mirror serving as a substrate for the ice condensation. With the combination of the closed-cycle helium refrigerator and a programmable temperature controller, the temperature of the silver mirror can be regulated precisely (±0.3 K) between 10 K and 350 K. The amorphous D_2O samples were formed by depositing D_2O onto the silver mirror at 12 K; the cubic crystalline D_2O samples were prepared by condensing D_2O vapor onto the silver substrate at 140 K and by cooling the samples to 12 K at 1.0 K min^{-1} after the deposition was complete. The thickness of the samples was estimated to 100 ± 30 nm based on the infrared absorption and the optical constants reported by Bergren et al. [21]; the day-to-day reproducibility of the ice condensation was within 5%. The samples were irradiated with 5 keV electrons at 12 K for 180 min at beam currents of 0 nA (blank experiment), 10 nA, 100 nA, 1000 nA, and 10 000 nA by scanning the electron beam over an area of 1.86 ± 0.02 cm^2. After each irradiation, the sample was kept at the same temperature for 60 min and then warmed up at 0.5 K min^{-1} to 293 K. The infrared spectra of the samples were measured *on-line* and *in-situ* by a Fourier transform infrared spectrometer (Nicolet 510 DX FTIR); the species subliming from the samples were monitored with a quadrupole mass spectrometer (Balzer QMG 420).

3. Results

3.1. Infrared spectra

Typical infrared spectra of D_2O ice before and after irradiation with 5 keV electrons at 1000 nA electron current are shown in Fig. 1. The patterns are similar to those observed in regular water ice (H_2O). Considering the spectrum of crystalline D_2O ice before the irradiation (Fig. 1), the absorption bands centered at 701 cm^{-1} and 1200 cm^{-1} correspond to the libration band (ν_L) and bending mode (ν_2), respectively. The absorption at 1635 cm^{-1} results from combination band ($\nu_L + \nu_2$) and/or libration overtone ($3\,\nu_L$). The peaks at 2305 cm^{-1} and 2572 cm^{-1} match the in-phase and out-of-phase symmetric stretch (ν_1) of the D_2 molecule; those at 2370 cm^{-1} and 2470 cm^{-1} originate from the transversal and longitudinal modes of asymmetric stretch vibration (ν_3). Note that the small peak at 827 cm^{-1} (Fig. 1) is due to a tiny amount of HDO resulted from the residual water in the vacuum system.

During the irradiation process, a new absorption feature centered at 2120 cm^{-1} emerged (Fig. 1) indicating the formation of D_2O_2. This feature is similar to the 2110 cm^{-1} peak in pure D_2O_2 ice [22]. Note that two additional absorption features of D_2O_2 were observed after most of the D_2O sublimed into the gas phase at about 178 K (Fig. 2). These peaks are centered at 1088 cm^{-1} and 1024 cm^{-1}. The 1088 cm^{-1} feature was identified as ν_2 symmetric bending of D_2O_2 molecule, whereas the 1024 cm^{-1} feature corresponds to the ν_6 asymmetric bending. The D_2O_2 ν_2 and ν_6 modes were found to be at 1060 and 1042 cm^{-1}, respectively, in pure D_2O_2 ice [22]. In our experiment, the frequency of the 2115 cm^{-1} feature is approximately the sum of the modes at 1088 cm^{-1} and 1024 cm^{-1}. Although Lannon et al. [22] assigned the 2110 cm^{-1} peak in their spectrum to the D_2O_2 $2\nu_6$ mode, here, we assign the 2115 cm^{-1} peak to the $\nu_2 + \nu_6$ combination mode of D_2O_2 molecule. The D_2O_2 absorption features overlap with the D_2O feature in both the amorphous ice and crystalline ices. It is difficult to compute the column densities of the D_2O_2 based on the infrared absorption.

3.2. Mass spectra

After the irradiation, the samples were held at the same temperature for one hour. Then, they were warmed up at a speed of 0.5 K min^{-1}. Fig. 3 presents the ion currents of various species as observed in the gas phase during the warm-up of the cubic crystalline D_2O ice. Most of the D_2O sublimed at about 179 K. Compared to the blank

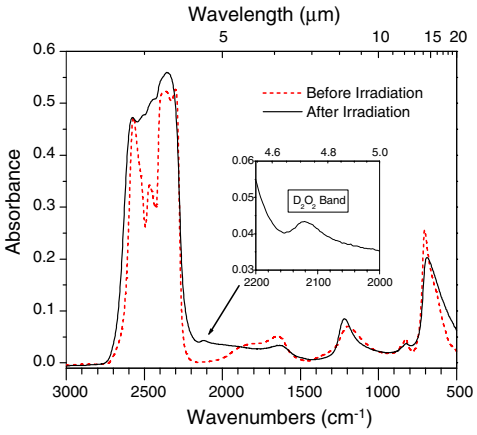

Fig. 1. Infrared spectra of cubic crystalline D_2O ice taken before (dashed line) and after the irradiation (solid line) at 12 K.

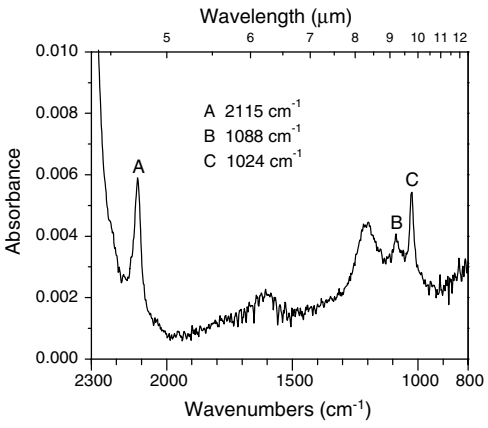

Fig. 2. Infrared spectrum of the irradiated sample taken in the warm-up phase at 178 K; most of the D2-water has sublimed. Peaks A, B, and C correspond to the $\nu_2 + \nu_6$ combination mode, ν_2 symmetric bending, and $\nu_2 + \nu_6$ asymmetric bending of D_2O_2, respectively. The remaining absorption features belong to D_2O ice.

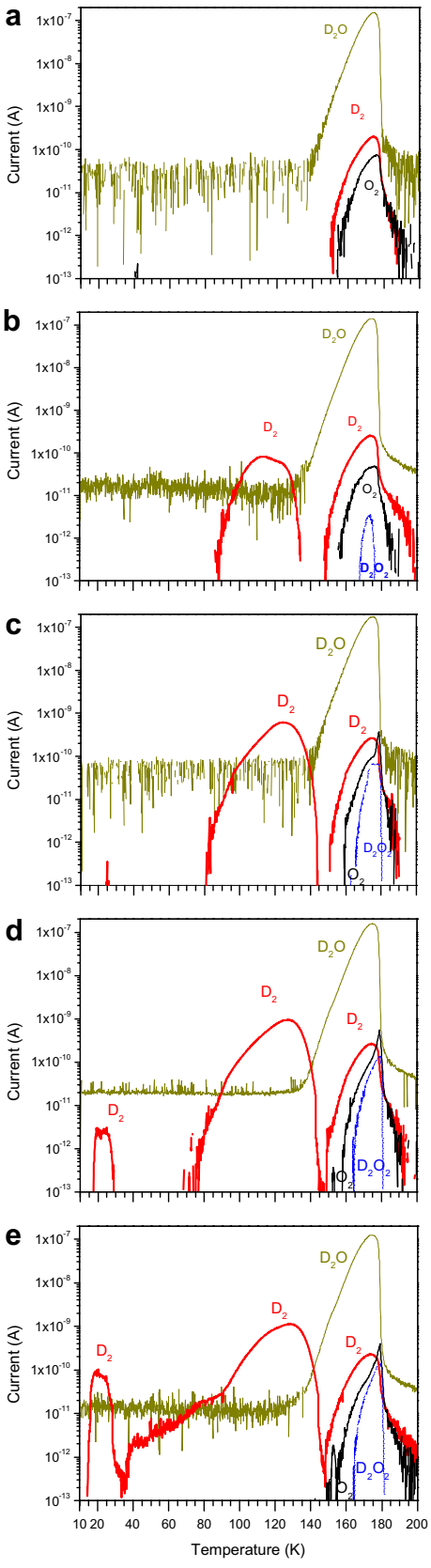

Fig. 3. Evolution of the ion currents of D_2, O_2, D_2O_2, and D_2O during the warm-up of cubic crystalline D_2O samples for irradiation experiments carried out with nominal electron currents of (a) 0, (b) 10, (c) 100, (d) 1000, and (e) 10 000 nA.

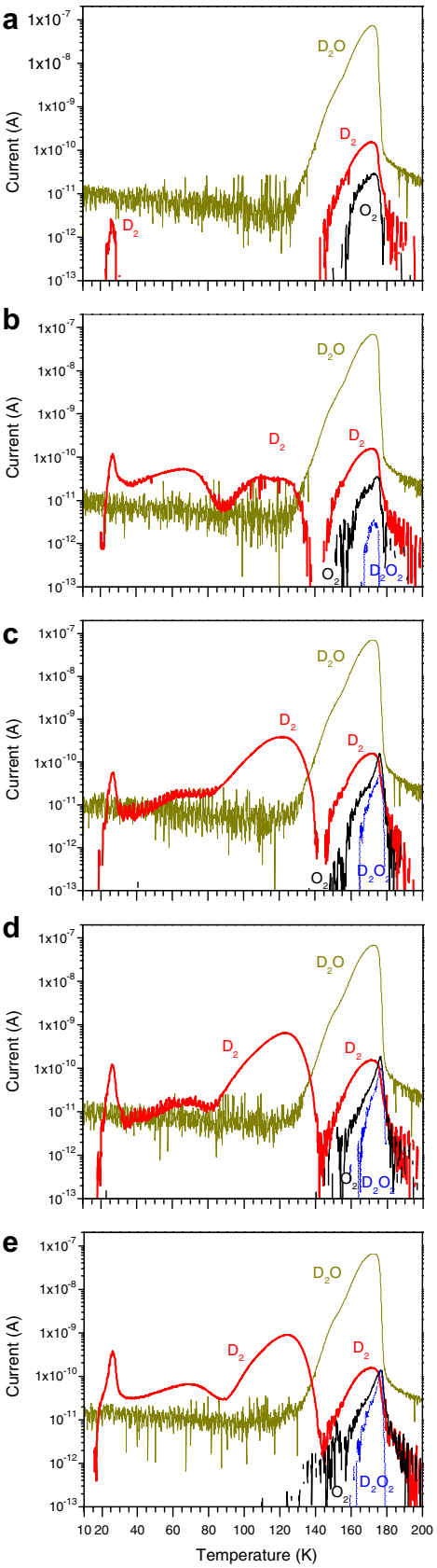

Fig. 4. Evolution of the ion currents of D_2, O_2, D_2O_2, and D_2O during the warm-up of amorphous D_2O samples for irradiation experiments carried out with nominal electron currents of (a) 0, (b) 10, (c) 100, (d) 1000, and (e) 10 000 nA.

experiment, the results also show that D_2, O_2, and D_2O_2 were generated during the irradiation and were released from the D_2O ices upon warming the samples. This is consistent with our previous experiments on regular water ice (H_2O) [15,16]. The newly formed D_2O_2 molecules were released at 163–181 K, whereas the oxygen molecules were liberated at 149–155 K. The release temperature of O_2 in D_2O is slightly higher than that in H_2O ice (147–151 K) [15]. Recall that molecular oxygen and deuterium signals in the blank experiment originate from ion–molecule reactions in the ionizer of the mass spectrometer [15]. The newly formed D_2 molecules were released between 80 K and 145 K. At currents of 1000 nA and 10 000 nA, additional weak D_2 peaks were also observed at 15–30 K. This early release of molecular deuterium likely originates from newly formed D_2 molecules close to the surface of D_2O ice.

The results from the amorphous samples are displayed in Fig. 4. The mass spectra of molecular oxygen and D_2O_2 are similar to those of the crystalline ice samples. The major differences are in the mass spectral profiles of D_2. Here, the D_2 peak at 80–145 K is similar to those of the irradiated crystalline ices. However, the amorphous blank (0 nA) experiment has a D_2 peak between 23 K and 29 K (Fig. 4a), which has not been observed in the crystalline experiments at 0, 10, 100 nA irradiation (Fig. 3a–c). This peak probably originates from the residual D_2 molecules adsorbed on the amorphous D_2O ice surface. It became stronger after the irradiation (Fig 4b–e), indicating that a fraction of the newly formed D_2 molecules migrated to or closer to the surface. In the mass spectra of amorphous D_2O ice, an additional broad D_2 peak also showed up at 30–80 K (Fig. 4b–e); this peak is absent in the crystalline ices. That peak probably arises from newly formed D_2 molecules trapped inside the pores of amorphous ices. Temperature annealing of amorphous ice between 30 K and 80 K causes the collapse of the micropores, thus, the D_2 molecules trapped inside were released. Laufer et al. [23] observed a similar peak in the experiment about D_2 molecules trapped in amorphous water (H_2O) ice.

In order to compare the production rates of the newly formed molecules in the crystalline versus the amorphous ice samples, the ion currents of the newly formed D_2, O_2, and D_2O_2 molecules were integrated and – accounting for the pumping speed and molecular masses – converted to the number of molecules synthesized (N) [15]. The data have been normalized with respect to the D_2O mass spectral intensities ($m/z = 20$) to correct the slightly different sample thicknesses at different days. The data are summarized in Table 1. The results in Table 1 indicate that the production rate of D_2 in amorphous ice is much higher than that in crystalline ice. We are able to tell that more O_2 and D_2O_2 were produced in amorphous ice than in crystalline ice. The difference between amorphous and crystalline ice became smaller at high electron currents, i.e., 1000 nA and 10 000 nA, when the irradiation was saturated. This is due to an effect of overlapping cascades [24] underlining that simulation experiments should be conducted at the lowest irradiation currents possible to mimic the dilute, extraterrestrial irradiation field effectively.

4. Discussion

Our experiments suggest that the structure of the water ice influences the production rates of molecular oxygen, molecular hydrogen, as well as hydrogen peroxide under irradiation. In order to understand the influence of the crystal structure on the formation rates, it is useful to recall how the newly-observed molecules are being synthesized. Similar to the H_2O system studied previously [15], we expect that D_2O can undergo an electron-induced unimolecular decomposition via Eqs. (1) and (2). The deuterium atoms can recombine to form molecular deuterium via reaction (3). D_2O_2 could be formed through recombination of two OD radicals (reaction (4)) or via electronically excited oxygen atoms reacting with water – either via insertion or through an oxywater intermediate (Eq. (5)). Molecular oxygen can be synthesized either by recombination of two oxygen atoms (reaction (6a)) or via decomposition of the oxywater intermediate (reaction (6b)) [25].

$$D_2O(X^1A_1) \rightarrow D(^2S_{1/2}) + OD(X^2\Pi_\Omega) \quad (1)$$

$$D_2O(X^1A_1) \rightarrow O(^1D) + D_2(X^1\Sigma_g^+) \quad (2)$$

$$D(^2S_{1/2}) + D(^2S_{1/2}) \rightarrow D_2(X^1\Sigma_g^+) \quad (3)$$

$$2OD(X^2\Pi_\Omega) \rightarrow D_2O_2(X^1A) \quad (4)$$

Table 1
The numbers of D_2, O_2, and D_2O_2 molecules (N) produced in cubic crystalline and amorphous D_2O ice by electron irradiation

Electron current (nA)	N (molecules)					
	Crystalline			Amorphous		
	D_2	O_2	D_2O_2	D_2	O_2	D_2O_2
0	0	0	0	0	0	0
10	1.5×10^{15}	>0	$>4.7\times10^{13}$	5.6×10^{15}	>0	$>9.1\times10^{13}$
100	9.1×10^{15}	>0	$>1.2\times10^{15}$	1.7×10^{16}	$>1.2\times10^{13}$	$>1.5\times10^{15}$
1000	1.6×10^{16}	$>9.2\times10^{11}$	$>2.1\times10^{15}$	2.6×10^{16}	$>1.9\times10^{13}$	$>2.3\times10^{15}$
10 000	2.5×10^{16}	$>1.2\times10^{13}$	$>2.6\times10^{15}$	3.7×10^{16}	$>1.4\times10^{14}$	$>2.8\times10^{15}$

The uncertainty of the numbers for D_2 is about ±20%.

$$O(^1D) + D_2O(X^1A_1) \rightarrow D_2O_2(X^1A) \quad (5a)$$

$$O(^1D) + D_2O(X^1A_1) \rightarrow [OOD_2(X^1A)] \rightarrow D_2O_2(X^1A) \quad (5b)$$

$$O(^3P) + O(^3P) \rightarrow O_2(X^3\Sigma_g^-) \quad (6a)$$

$$D_2OO(X^1A) \rightarrow O_2(a^1\Delta_g) + D_2(X^1\Sigma_g^+) \quad (6b)$$

Besides the reaction channels to form new products, the D and OD fragment can also recombine to form D_2O molecules via reaction (7). This is a very important competing pathway that influences the production rates of D_2, O_2, and D_2O_2.

$$D(^2S_{1/2}) + OD(X^2\Pi_\Omega) \rightarrow D_2O(X^1A_1) \quad (7)$$

Recall that in our recent study of the temperature-dependence of the electron irradiation of crystalline water ice [16], we found that the production rates of H_2, O_2 and H_2O_2 decrease as the temperature rises. We suggested that is due to the enhanced recombination rates of H and OH fragments at higher temperature, i.e., a temperature dependent, diffusion controlled reaction pathway. In the present work, the formation rates of D_2, O_2, and D_2O_2 are systematically higher in the amorphous ice samples. This could be due to the lower recombination rate of D and OD fragments in the amorphous ice; this low recombination rate could be the result of pores inside amorphous ice which actually limit the diffusion and reaction (7) of the atoms/radicals in the amorphous ices. As soon as a D_2O molecule close to the pores is dissociated via reaction (1) for example, the D or OD fragments may diffuse quickly into the empty space in the pores, therefore, reducing the chances for the D and OD fragments to recombine with each other. Andersson et al. [26] carried out a molecular dynamics study on the photodissociation of water in crystalline (I_h) ice. The authors found that the desorption of H atoms decreases from the first bilayer to the third bilayer; the fractions of trapped H and OH species increase from the first bilayer to the third bilayer; the corresponding H + OH recombination was also found to increase from the first to the third bilayer. According to momentum conservation, most of the excess kinetic energy is obtained by the D atom when a D_2O molecule is dissociated to D and OD via Eq. (1). The D atoms from the first molecular layer around the cavities will be able to escape easily into the empty space in the cavities and can diffuse around the cavity walls to encounter a second D atom forming D_2. A fraction of the D atoms from the inner layers will also be able to escape to the cavities. Therefore, the D + OD recombination is likely reduced by the escaping of D atoms into the micropores. In crystalline D_2O, the fraction of D and OD recombination via reaction (7) is much higher due to the lack of micro pores. An alternative explanation of an enhanced production of, for instance, D_2O_2, could be the existence of lattice defects in amorphous water. Bednarek et al. [27] found a higher yield of trapped HO_2 radicals in hyperquenched glassy water γ-irradiated at 77 K. They suggested that is the result of a high concentration of L-defects in glassy water. Since L-defects exist in amorphous water, but not cubic crystalline water ice, it is possible that these L-defects also contribute to the higher production rates of D_2O_2 in the amorphous D_2O ice. Here, the L-defects favor a recombination geometry of the OD radicals. In detail, L-defects have two D2-water molecules orientated in this way so that the oxygen atoms of the water molecules neighbor each other, i.e., the existence of $[D_2O\cdots OD_2]$ defects. Here, as soon as an impinging high energy electron ruptures the O–D bonds of two neighboring D_2O molecules in the L-defect geometry, a recombination of the OD radicals to D_2O_2 is favorable. This is in strong contrast to crystalline water, in which the oxygen atom of each water molecule is bonded via hydrogen bridge bonding to a neighboring water molecule, i.e., $[DOD\cdots OD_2]$. This geometry could make the recombination of two OD fragments less likely compared to L-defects. Finally, we would like to point out that Grieves and Orlando [10] conducted similar studies on the electron stimulated generation and trapping of D_2 and O_2 in amorphous and crystalline D_2O ices. In their experiments, the irradiation was conducted at 55 K utilizing 100 eV electrons; the species released into the gas phase were monitored with a quadrupole mass spectrometer during the warm up process. These experiments showed that porous amorphous ice exhibits higher yields of D_2 and O_2.

5. Summary and astrophysical implications

With the combination of the previous works on crystalline H_2O ice [15,16] and this work on D_2O ice, we can conclude that the production rates of H_2, O_2 and H_2O_2 in irradiated crystalline water ice decrease with increasing temperature, and the productions rates in amorphous ice are higher than those in the crystalline ice. Since the surfaces of dust grains in cold molecular clouds and of objects in Oort cloud are predominantly low temperature (10 K) amorphous water ice, the concentrations of molecular hydrogen, molecular oxygen, and hydrogen peroxide is expected to be higher than those on the surfaces of Kuiper Belt Objects such as Quaoar where crystalline water dominates [28] if they have similar compositions and irradiation exposure. Bar-Nun and Prialnik [29] suggested a potential existence of a hydrogen coma around comets at heliocentric distances larger than 4 AU. Our mass spectrometric results support the idea that molecular hydrogen stored in the pores of the amorphous water ice can be released when the comets originated from Oort cloud first approach the Sun.

Acknowledgements

This work was financed by the NASA Astrobiology Institute under Cooperative Agreement NNA04CC08A at the University of Hawaii at Manoa (WZ, DJ) and by the US National Science Foundation (NSF; AST-0507763; DJ, RIK). We are grateful to Ed Kawamura (University

of Hawaii at Manoa, Department of Chemistry) for his electrical work.

References

[1] R.A. Baragiola, Planet Space Sci. 51 (2003) 953.
[2] R.E. Johnson, T.I. Quickenden, J. Geophys. Res.-Planets 102 (1997) 10985.
[3] R.E. Johnson, P.D. Cooper, T.I. Quickenden, G.A. Grieves, T.M. Orlando, J. Chem. Phys. 123 (2005) 184715.
[4] M.J. Loeffler, R.A. Baragiola, Geophys. Res. Lett. 32 (2005) L17202.
[5] N.G. Petrik, A.G. Kavetsky, G.A. Kimmel, J. Chem. Phys. 125 (2006) 124702.
[6] J. Bergeld, D. Chakarov, J. Chem. Phys. 125 (2006) 141103.
[7] N. Watanabe, T. Horii, A. Kouchi, Astrophys. J. 541 (2000) 772.
[8] M.T. Sieger, W.C. Simpson, T.M. Orlando, Nature 394 (1998) 554.
[9] T.M. Orlando, M.T. Sieger, Surf. Sci. 528 (2003) 1.
[10] G.A. Grieves, T.M. Orlando, Surf. Sci. 593 (2005) 180.
[11] M.H. Moore, R.L. Hudson, Icarus 145 (2000) 282.
[12] D.A. Bahr, M. Fama, R.A. Vidal, R.A. Baragiola, J. Geophys. Res.-Planets 106 (2001) 33285.
[13] O. Gomis, G. Leto, G. Strazzulla, Astron. Astrophys. 420 (2004) 405.
[14] M.J. Loeffler, U. Raut, R.A. Vidal, R.A. Baragiola, R.W. Carlson, Icarus 180 (2006) 265.
[15] W. Zheng, D. Jewitt, R.I. Kaiser, Astrophys. J. 639 (2006) 534.
[16] W. Zheng, D. Jewitt, R.I. Kaiser, Astrophys. J. 648 (2006) 753.
[17] P. Jenniskens, D.F. Blake, Science 265 (1994) 753.
[18] J.K. Davies, T.L. Roush, D.P. Cruikshank, M.J. Bartholomew, T.R. Geballe, T. Owen, C. de Bergh, Icarus 127 (1997) 238.
[19] H. Kawakita et al., Astrophys. J. 601 (2004) L191.
[20] C.J. Bennett, C. Jamieson, A.M. Mebel, R.I. Kaiser, Phys. Chem. Chem. Phys. 6 (2004) 735.
[21] M.S. Bergren, D. Schuh, M.G. Sceats, S.A. Rice, J. Chem. Phys. 69 (1978) 3477.
[22] J.A. Lannon, F.D. Verderame, J.R.W. Anderson, J. Chem. Phys. 54 (1971) 2212.
[23] D. Laufer, E. Kochavi, A. Bar-Nun, Phys. Rev. B – Condens. Matter 36 (1987) 9219.
[24] R.I. Kaiser, K. Roessler, Astrophys. J. 475 (1997) 144.
[25] Y. Ge, K. Olsen, R.I. Kaiser, J.D. Head, ASTROCHEMISTRY: From Laboratory Studies to Astronomical Observations, AIP, Honolulu, HI, USA, 2006, p. 253.
[26] S. Andersson, G.-J. Kroes, E.F. van Dishoeck, Chem. Phys. Lett. 408 (2005) 415.
[27] J. Bednarek, A. Plonka, A. Hallbrucker, E. Mayer, M.C.R. Symons, J. Am. Chem. Soc. 118 (1996) 9387.
[28] D.C. Jewitt, J. Luu, Nature 432 (2004) 731.
[29] A. Bar-Nun, D. Prialnik, Astrophys. J. 324 (1988) L31.